JOC The Journal of Organic Chemistry

Article

pubs.acs.org/joc

Theoretical Study on the Conformation and Aromaticity of Regular and Singly N-Confused [28]Hexaphyrins

Motoki Toganoh[†] and Hiroyuki Furuta*[,†,‡]

[†]Department of Chemistry and Biochemistry, Graduate School of Engineering, and [‡]Center for Molecular Systems, Kyushu University, 744 Moto-oka, Nishi-ku, Fukuoka 819-0395, Japan

Supporting Information

ABSTRACT: Structures and electronic states of regular and singly N-confused [28]hexaphyrins(1.1.1.1.1.1) were thoroughly studied with the aid of DFT calculations. To obtain systematic information, all the conceivable structures (450 structures in total) were examined. Unlike the [26]hexaphyrins(1.1.1.1.1.1) reported previously (*J. Org. Chem.* **2010**, 75, 8213−8223), the electronic states of [28]hexaphyrins were highly affected by their conformations. The planar conformers (dumbbell, rectangular, triangular) show Hückel antiaromaticity, while the singly twisted conformers show Möbius aromaticity. Figure-eight structures correspond to the doubly twisted structures and show nonaromaticity. Disruption of annulenic circuits in singly N-confused [28]hexaphyrins caused weakening of both aromatic and antiaromatic characteristics. Relative stabilities among conformers were mainly governed by the intramolecular hydrogen bonds and secondarily affected by the steric factors. In addition, interconversion pathways among conformers were proposed on the basis of calculations on singly N-confused [28]hexaphyrins.

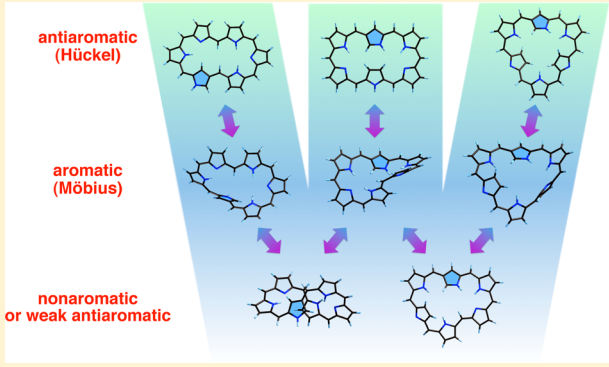

INTRODUCTION

In porphyrins and related compounds, and π-conjugated macrocyclic compounds in general, the conformation or molecular shape plays a critical role in their properties as well as reactivities.[1,2] Especially in the case of expanded porphyrins, molecular skeletons become very flexible and a variety of molecular shapes must be taken into account to understand their electronic properties.[3] Thus, control of the conformation and comprehension of the structure−property relationship is an important subject to address. Conventional methods to control the molecular conformation in expanded porphyrins rely on covalent bonding as well as metal coordination.[2] Alternatively, we have recently developed an N-confusion strategy to control molecular shapes in porphyrin-related macrocycles.[4]

Efficacy of the N-confusion strategy was distinctively demonstrated in a series of [26]hexaphyrins(1.1.1.1.1.1). Rectangular conformations could be stabilized by single[5] or double[6] N-confusion, and triangular conformations could be stabilized by triple N-confusion.[7] Important factors governing the molecular conformation in [26]hexaphyrins were revealed to be intramolecular hydrogen bonds as well as steric repulsions imposed by the peripheral substituents.[8]

One of the important properties of expanded porphyrins is their variable aromaticity. In the porphyrinoids, the number of π-electrons could be readily tuned by the number of NH protons without changing the molecular skeleton. Common tetrapyrrolic porphyrins possessing two NH protons have an 18π annulenic circuit and usually take a planar conformation to exhibit Hückel aromaticity. By oxidation or reduction, 16π porphyrin (no NH proton)[9] or 20π porphyrin (four NH protons)[10] can be synthesized, but they are often less stable and are still rare. In contrast, such a 4*n*-π-electron system becomes much more stable and common in expanded porphyrins.[2] Because of their wide availability from the viewpoint of synthetic organic chemistry, hexaphyrins are one of the most studied macrocycles with regard to the 4*n*-π-electron system.[11] Standard hexaphyrin has 26 π-electrons and shows Hückel aromaticity. Although a variety of conformations such as dumbbell, rectangular, figure-eight, and triangular were observed for [26]hexaphyrins, all conformers commonly show Hückel aromaticity.[8,12]

On the other hand, the aromaticity of [28]hexaphyrins, which could be prepared readily by the reduction of [26]hexaphyrins and are stable under ambient conditions, is highly affected by their conformations. Namely, rectangular conformers show Hückel antiaromaticity,[13] twisted rectangular conformers show Möbius aromaticity,[14,15] and figure-eight conformers show weak antiaromaticity or nonaromaticity.[16−18] Thus, a detailed study on the relationship between conformation and electronic structure in [28]hexaphyrins is needed.

The importance of a theoretical study on expanded porphyrins is derived from their bewildering structural diversity.

Received: July 14, 2013
Published: August 25, 2013

dx.doi.org/10.1021/jo401531w | *J. Org. Chem.* 2013, 78, 9317−9327

Chart 1. Representative Conformations of [28]Hexaphyrins

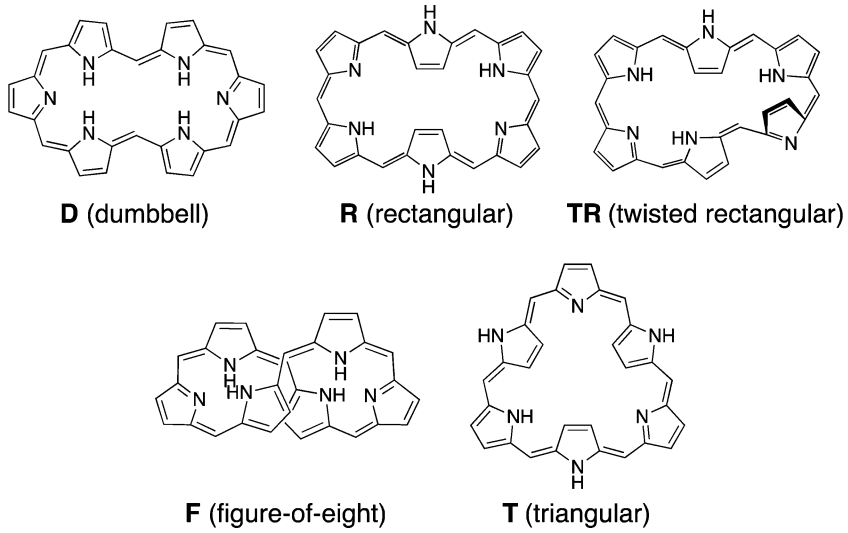

Thousands of structures can be drawn even for a single skeleton owing to the conformation, tautomerization, and confusion. Consequently, expanded porphyrins can exist as a mixture of many conformers, tautomers, and regioisomers, especially in solution. Thus, as well as the spectroscopic data, the theoretical information on each structure would be of great help for the better understanding of their properties. Actually, a theoretical study on a series of N-confused [26]hexaphyrins gave us plenty of information useful for spectroscopic analyses and further molecular design.[3,8] In this study, we theoretically investigated the regular and singly N-confused [28]hexaphyrins to reveal the factors that govern their conformations and electronic states.

CALCULATION DETAILS

General Procedures. All DFT calculations were performed with the Gaussian09 program package.[19] The basis sets implemented in the program were used. The B3LYP density functional method[20] was used with the 6-31G** basis set for structural optimizations as well as frequency analyses. The 6-311++G** basis set was used for nucleus-independent chemical shift (NICS)[21] calculations. Initial structures have been arbitrarily constructed. Equilibrium geometries were fully optimized and verified by the frequency calculations, where no imaginary frequency was found. The NICS values were calculated with a gauge invariant atomic orbitals (GIAO) method at the center of the 36 heavy atoms constructing the hexaphyrin framework of the optimized structure.

Structures. Regular [28]hexaphyrin (N0Hex-28) and singly N-confused [28]hexaphyrin (N1Hex-28) were subjected to DFT calculations. Here only the hexaphyrin(1.1.1.1.1.1) framework was treated, although many interesting members of the hexaphyrin family were reported.[22] On the basis of the previous studies, five conformations were mainly treated, namely, dumbbell (D), rectangular (R), twisted rectangular (TR), figure-eight (F), and triangular (T), as shown in Chart 1. The twisted rectangular conformation is often called the Möbius conformation, but it is named in such a way here to represent its shape.[23] For each conformation, all the possible NH tautomers were taken into consideration. In addition, all the possibilities for the position and direction of the N-confused pyrrole were examined in the singly N-confused [28]hexaphyrins. Each structure is denoted by a combination of compound and conformation regardless of the tautomers and positions of the N-confused pyrrole, such as N0Hex-28-D, N1Hex-28-TR, and so on. Some starting structures did not have a local minimum point and were transformed into the other structure through optimization. This issue will be discussed in a later section.

The NH tautomers are classified according to the intramolecular hydrogen-bonding index (N_H), which was defined in the previous study (Figure 1).[8] One dipyrromethene unit corresponds to $N_H = 1$ (**A**). When two dipyrromethene units share one pyrrole ring in common as in **B** or **C**, $N_H = 1.5$.

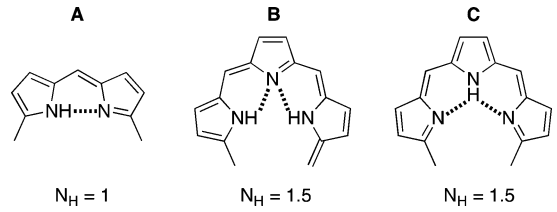

Figure 1. Definition of the intramolecular hydrogen-bonding index (N_H).

The representative optimized structures for [28]hexaphyrin conformers are shown in Figure 2. Basically, the dumbbell, rectangular, figure-eight, and triangular conformers of [28]hexaphyrin have structures similar to those of [26]hexaphyrin, but the dumbbell conformer of [28]hexaphyrin is distorted from planarity, while that of [26]hexaphyrin is almost planar. The twisted rectangular structure is derived from the rectangular structure by rotating the center pyrrole ring on the long side. No significant differences are observed in the optimized structures between the regular and singly N-confused [28]hexaphyrins in each conformer.

Regular [28]hexaphyrins always have completed [28]annulenic circuits regardless of the positions of the NH protons. Meanwhile, in singly N-confused [28]hexaphyrins, [28]annulenic circuits are completely connected or disrupted depending on the positions of the NH protons. Since the presence of an annulenic circuit affects the electronic state of hexaphyrins,[5b] it is clearly illustrated by colors (Figure 3). Completed annulenic circuits are drawn in bold magenta (circuit-on), and disrupted annulenic circuits are drawn in bold black (circuit-off). To clarify the presence or absence of a completed circuit, circuit-on is indicated by -C and circuit-off is indicated by -N as in N0Hex-28-R-C and N1Hex-28-R-N.

RESULTS AND DISCUSSION

Relative Energies of Regular [28]Hexaphyrins. The relative energies of the conformers and NH tautomers of regular [28]hexaphyrins are summarized in Figure 4. A vertical axis corresponds to the relative energies, and each symbol represents one NH tautomer. Roughly speaking, NH

dx.doi.org/10.1021/jo401531w | J. Org. Chem. 2013, 78, 9317−9327

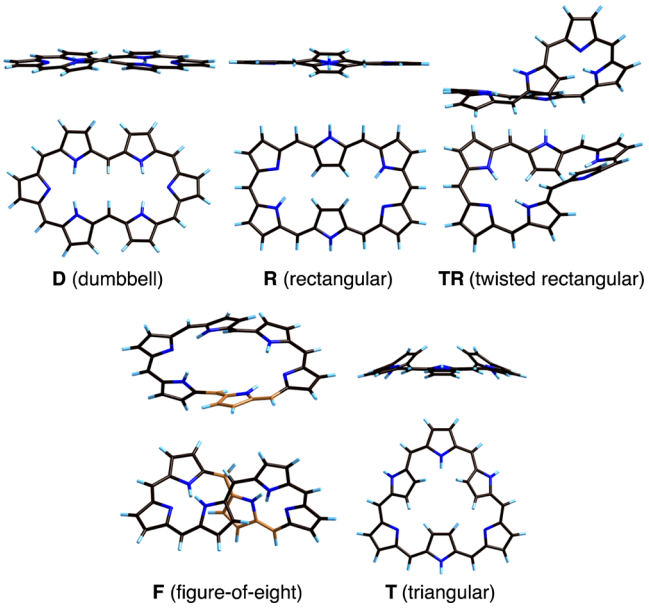

Figure 2. Three-dimensional structures of the representative [28]-hexaphyrin conformers.

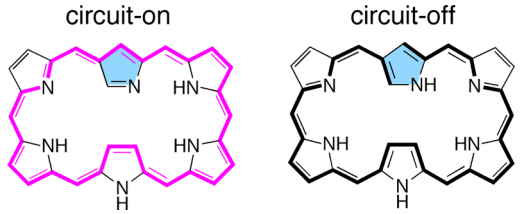

Figure 3. Completed and disrupted [28]annulenic circuits of singly N-confused [28]hexaphyrins.

tautomerism in each conformer causes an energy difference of 10−30 kcal/mol, suggesting the positions of the NH protons are a critical factor to control their relative stability. In this section, the most stable NH tautomers in each conformer will be discussed. Among five conformers, a dumbbell structure (N0Hex-28-D) is the most stable and shows Hückel antiaromaticity (NICS = 37.39 ppm). Although a twisted rectangular structure (N0Hex-28-TR) shows Möbius aromaticity (NICS = −14.93 ppm), it is less stable than antiaromatic N0Hex-28-D by 6.72 kcal/mol. A rectangular structure (N0Hex-28-R) shows strong antiaromaticity (NICS = 46.98 ppm) but is less stable than N0Hex-28-D by 9.21 kcal/mol. A figure-eight structure (N0Hex-28-F) shows nearly nonaromatic character (NICS = 7.80 ppm). Its thermodynamic stability is similar to that of N0Hex-28-R. A triangular structure (N0Hex-28-T) is much less stable than the other conformers and shows moderate antiaromaticity (NICS = 17.22 ppm).

Relative Energies of Singly N-Confused [28]-Hexaphyrins. The relative energies for the conformers and NH tautomers of singly N-confused [28]hexaphyrins are summarized in Figure 5. The most stable NH tautomers in each conformer are discussed in the same manner as the regular [28]hexaphyrins. Among all conformers, a rectangular structure (N1Hex-28-R) is most stable, which is in sharp contrast to the regular [28]hexaphyrins. Since its annulenic circuit is disrupted, N1Hex-28-R shows nearly nonaromatic character (NICS = 7.36 ppm). A dumbbell structure (N1Hex-28-D) is less stable than N1Hex-28-R by 3.39 kcal/mol and shows weak antiaromaticity (NICS = 9.97 ppm). A twisted rectangular structure (N1Hex-28-TR) shows distinctive Möbius aromaticity (NICS = −10.98 ppm), but is slightly less stable than N1Hex-28-R and N1Hex-28-D. A figure-eight structure (N1Hex-28-F) and a triangular structure (N1Hex-28-T) are much less stable by 14−18 kcal/mol than the other conformers. The former is nonaromatic (NICS = −0.79 ppm), and the latter is moderately antiaromatic (NICS = 18.41 ppm).

Intramolecular Hydrogen Bonds. Intramolecular hydrogen bonds or N_H values in [28]hexaphyrins significantly affected their relative stability regardless of the conformations similarly to those in [26]hexaphyrins.[8] Figures 6 and 7 summarize the relationship between the relative stabilities and the N_H values in the regular and singly N-confused [28]-hexaphyrins, respectively. The plots are classified according to the conformations. While other factors such as intramolecular steric repulsions and ring strain should be changed also by NH tautomerization even in the same conformers, they could be counterbalanced with regression analysis. Thus, only the entire trend imposed by the intramolecular hydrogen bonds will be discussed roughly in this section. In the dumbbell (r = 0.9675), rectangular (r = 0.9864), twisted rectangular (r = 0.9770), and figure-eight (r = 0.9738) structures of regular [28]hexaphyrins, formation of one hydrogen bond (N_H = 1) could help to

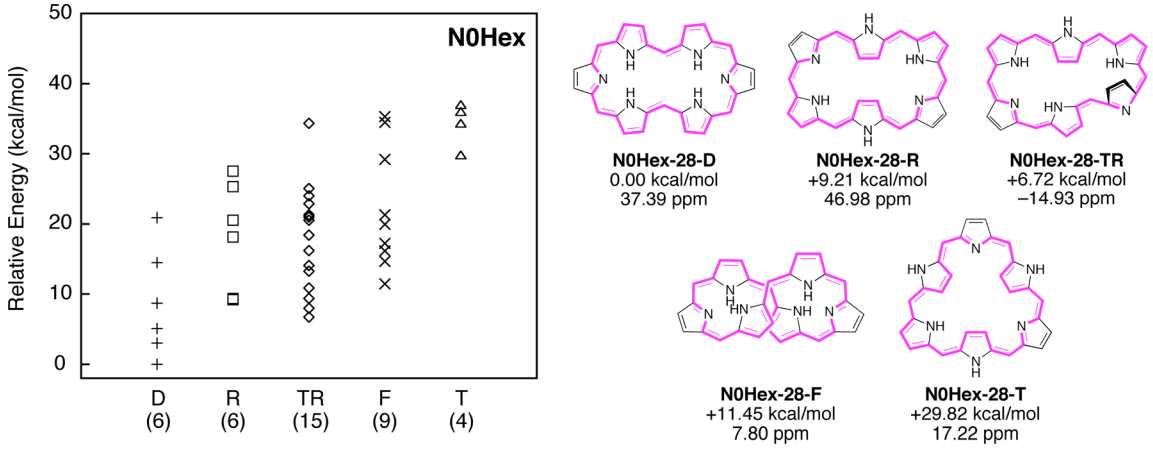

Figure 4. Relative energies of regular [28]hexaphyrin conformers and NH tautomers. The numbers in parentheses indicate the number of calculated tautomers. The structures, relative energies, and NICS values of the most stable tautomers are shown on the right.

dx.doi.org/10.1021/jo401531w | J. Org. Chem. 2013, 78, 9317−9327

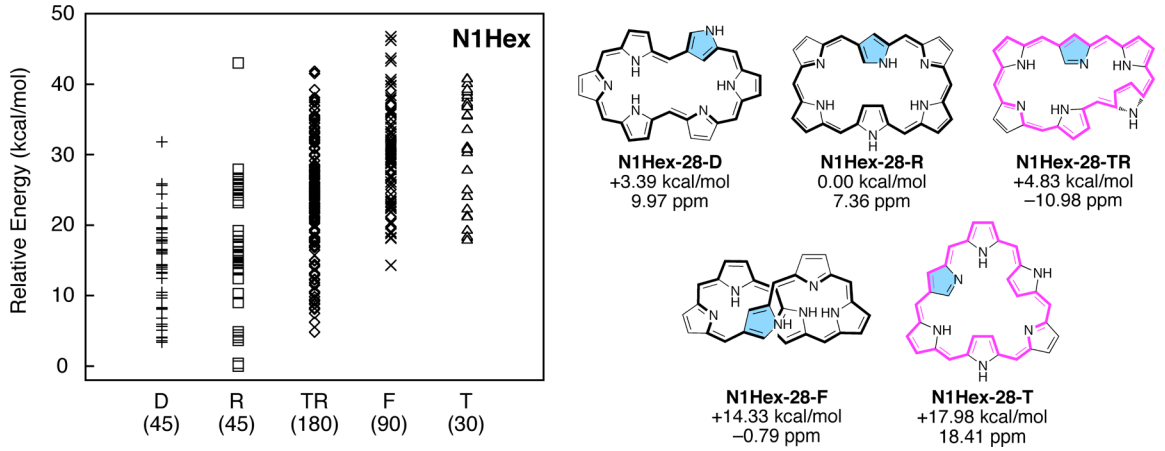

Figure 5. Relative energies of singly N-confused [28]hexaphyrin conformers and NH tautomers. The numbers in parentheses indicate the number of calculated tautomers. The structures, relative energies, and NICS values of the most stable tautomers are shown on the right.

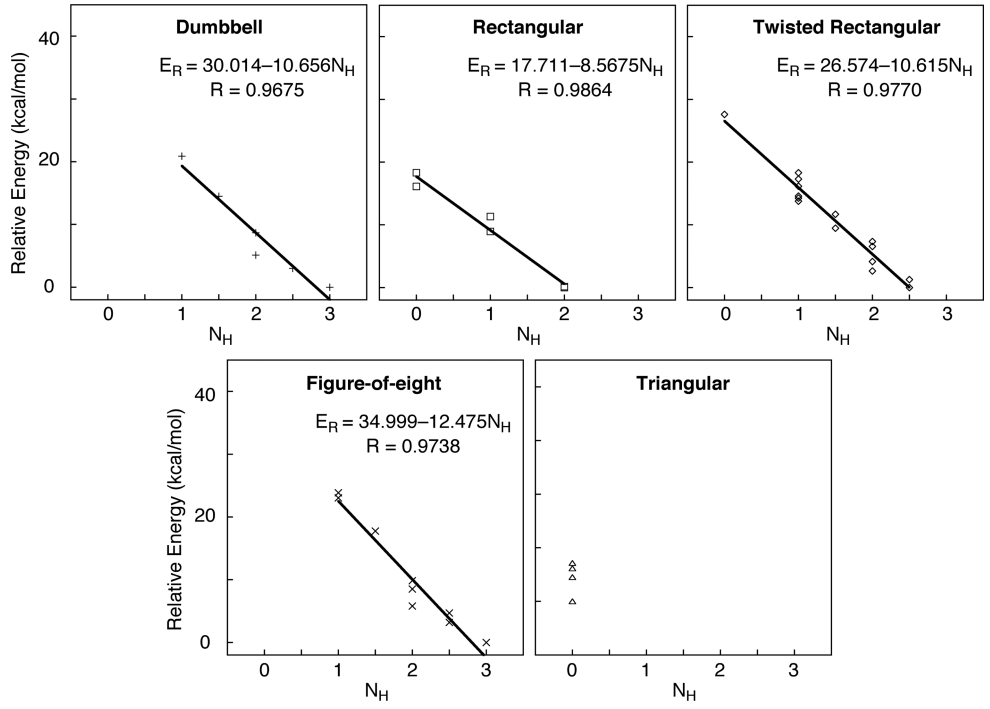

Figure 6. Relative energies and hydrogen-bonding indices of regular [28]hexaphyrin conformers with the regression lines.

stabilize the macrocycle by ca. 10 kcal/mol with high correlations. The triangular structures could not be analyzed due to the absence of variation in the N_H values. In the case of singly N-confused [28]hexaphyrins, on the other hand, the dumbbell (r = 0.9453), rectangular (r = 0.9360), twisted rectangular (r = 0.8160), and figure-eight (r = 0.9311) structures showed lower correlations than those of regular [28]hexaphyrins, although a similar stabilization effect by ca. 10 kcal/mol per N_H was observed. This lower correlation might mean that the position of the N-confused pyrrole ring affects the relative stability to some degree.

Evaluation of Ring Strain. Usually, ring strain of macrocyclic compounds is discussed from the viewpoints of many factors such as abnormal bond lengths, abnormal bond angles, unfavorable dihedral angles, and transannular repulsions.[24] Since the bond lengths and bond angles are normal and transannular repulsions are not observed in unsubstituted hexaphyrins, dihedral angles are focused on for the evaluation of ring strain in this study. As utilized in the previous study,[8] averaged dihedral angles between the neighboring two pyrrole rings are chosen as the reference parameter for the ring strain.

The dihedral angles between the neighboring pyrrole rings (Φ_p) and their average (Φ_{av}) and relative energies among 10 structures (ΔE_{all}) are summarized in Table 1. Generally, the correlation between Φ_{av} and ΔE_{all} seems lower. For example, the stability of N0Hex-28-TR (ΔE_{all} = +6.72 kcal/mol) and N0Hex-28-F (ΔE_{all} = +11.45 kcal/mol) is moderate in spite of their large Φ_{av} values (32.10° and 31.48°). The same trend is also found in singly N-confused [28]hexaphyrins. This is in contrast to the case of [26]hexaphyrins, where a high correlation between Φ_{av} and the relative energies is observed. In the [26]hexaphyrins, planarity of the macrocycle should be important to keep effective π-orbital overlap for aromaticity, whereas planarity becomes less important in non- or

dx.doi.org/10.1021/jo401531w | J. Org. Chem. 2013, 78, 9317−9327

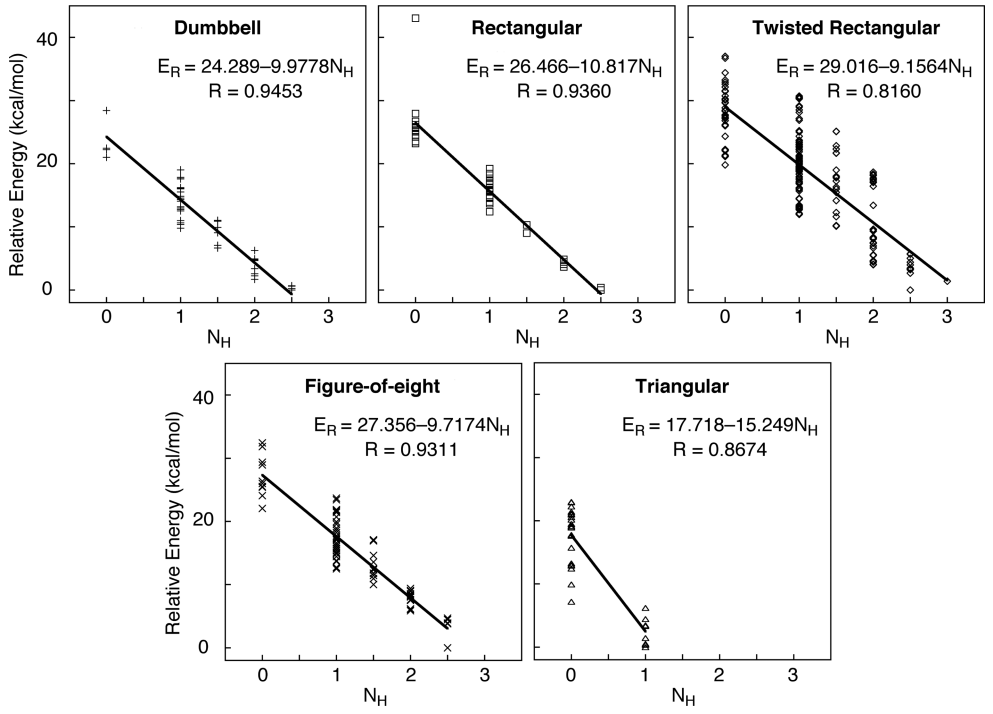

Figure 7. Relative energies and hydrogen-bonding indices of singly N-confused [28]hexaphyrin conformers with the regression lines.

Table 1. Dihedral Angles between the Neighboring Pyrrole (Φ_P) Rings and Their Average (Φ_{av}) and Relative Energies (ΔE_{all}) of the Most Stable NH Tautomers in Hexaphyrins[a]

structure	Φ_P (deg)						Φ_{av}(deg)	ΔE_{all} (kcal/mol)	N_H
N0Hex-28-D	3.24	2.51	24.61	7.38	6.08	20.92	10.79	0.00	3
N0Hex-28-R	2.18	15.28	16.74	2.17	15.26	16.73	11.39	9.21	2
N0Hex-28-TR	35.90	46.31	32.50	31.88	9.14	36.84	32.10	6.72	2.5
N0Hex-28-F	16.86	55.68	21.86	16.86	55.72	21.87	31.48	11.45	3
N0Hex-28-T	30.75	29.76	18.25	18.25	29.76	30.75	26.25	29.82	0
N1Hex-28-D	14.78	4.17	21.31	9.99	9.32	18.18	12.96	7.95	2.5
N1Hex-28-R	5.06	18.09	19.59	3.13	8.29	5.30	9.91	4.55	2.5
N1Hex-28-TR	35.37	47.19	28.89	38.37	30.11	18.67	33.10	9.38	2.5
N1Hex-28-F	15.69	40.23	39.54	17.76	22.44	49.88	30.92	18.88	2.5
N1Hex-28-T	31.87	23.01	24.93	17.78	4.19	17.29	19.85	22.53	1

[a]Hydrogen-bonding indices (N_H) are also shown.

antiaromatic [28]hexaphyrins. Rather, twisted structures could stabilize the macrocycles in the case of Möbius aromatic [28]hexaphyrins.

Aromaticity and Orbital Degeneracy. The aromaticity of [28]hexaphyrins was evaluated from the viewpoint of the NICS, harmonic oscillator model of aromaticity (HOMA),[25] HOMO−LUMO gap (ΔE_{HL}), and orbital degeneracy. The NICS values, HOMA indices, and ΔE_{HL} values of [28]-hexaphyrins are listed in Table 2. The NICS values were calculated at the center of 36 heavy atoms composing the hexaphyrin main framework. The HOMA indices were estimated along the annulenic circuit shown with bold lines. In the dumbbell conformations, the NICS values indicate that N0Hex-28-D-C (37.39 ppm) and N1Hex-28-D-C (33.59 ppm) have strong antiaromaticity, while N1Hex-28-D-N (9.97 ppm) has weak antiaromaticity. Accordingly, N0Hex-28-D-C (1.09 eV) and N1Hex-28-D-C (1.10 eV) show very narrow HOMO−LUMO gaps, while N1Hex-28-D-N (1.36 eV) shows a relatively wide HOMO−LUMO gap. Nevertheless, all three structures show almost the same HOMA indices of around

Table 2. NICS Values, HOMA Indices, and HOMO−LUMO Gaps of [28]Hexaphyrins

structure	NICS (ppm)	HOMA	ΔE_{HL} (eV)
N0Hex-28-D-C	37.39	0.6797	1.09
N1Hex-28-D-C	33.59	0.6923	1.10
N1Hex-28-D-N	9.97	0.6909	1.36
N0Hex-28-R-C	46.98	0.7063	1.03
N1Hex-28-R-C	20.96	0.7283	1.21
N1Hex-28-R-N	7.36	0.7023	1.47
N0Hex-28-TR-C	−14.93	0.8183	1.95
N1Hex-28-TR-C	−10.98	0.8136	1.79
N1Hex-28-TR-N	−6.78	0.7466	1.73
N0Hex-28−F-C	7.80	0.6359	1.39
N1Hex-28−F-C	2.30	0.6521	1.47
N1Hex-28−F-N	−0.79	0.6695	1.56
N0Hex-28-T-C	17.22	0.6540	1.31
N1Hex-28-T-C	18.41	0.6664	1.24
N1Hex-28-T-N	9.15	0.6851	1.39

dx.doi.org/10.1021/jo401531w | J. Org. Chem. 2013, 78, 9317−9327

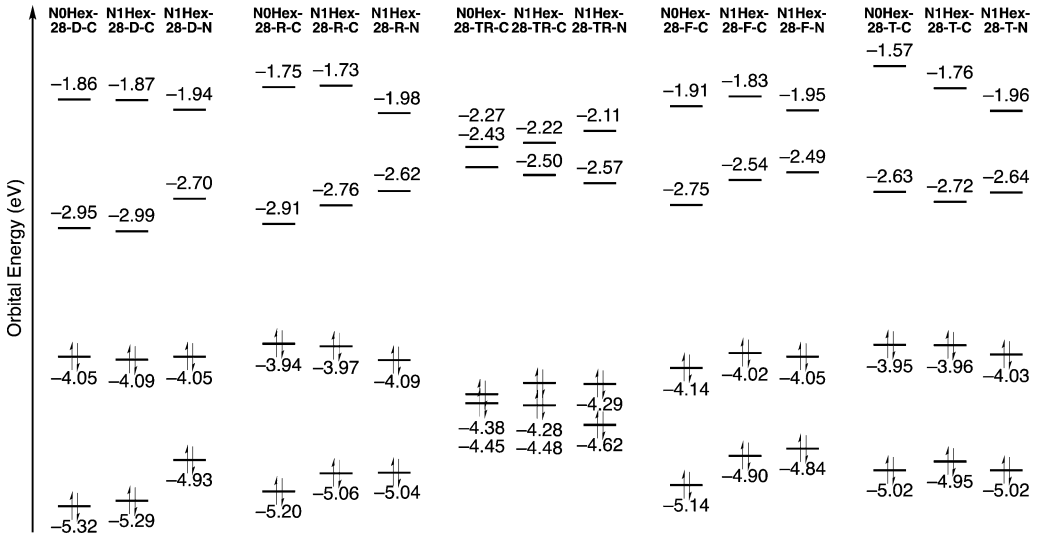

Figure 8. HOMO, HOMO − 1, LUMO, and LUMO + 1 energy diagrams of [28]hexaphyrins.

Table 3. Comparison of Relative Energies (kcal/mol) between Regular and Singly N-Confused [28]Hexaphyrins with the Same Conformation and the Same N_H Value

	N_H = 0	N_H = 1	N_H = 1.5	N_H = 2	N_H = 2.5	N_H = 3
N0Hex-28-D		20.90	14.49	5.12	3.01	0.00
		(0.94)	(−0.48)	(−4.86)	(−1.98)	(0.00)
N1Hex-28-D	28.98	17.74	14.60	9.64	7.95	
	(−0.95)	(−2.22)	(−0.37)	(−0.34)	(2.96)	
N0Hex-28-R	20.77	13.60		4.65		
	(−6.27)	(−2.63)		(−0.76)		
N1Hex-28-R		12.40	9.00	4.43	0.00	
		(−3.83)	(−1.82)	(−0.98)	(0.00)	
N0Hex-28-TR	27.62	13.78	9.46	2.64	0.00	
	(0.15)	(−4.53)	(−4.27)	(−6.52)	(−4.58)	
N1Hex-28-TR	22.45	14.65	12.78	6.66	2.66	4.05
	(−5.02)	(−3.66)	(−0.95)	(−2.50)	(−1.92)	(4.05)
N0Hex-28-F		23.03	17.75	5.80	3.21	0.00
		(−3.60)	(−3.18)	(−3.91)	(−1.65)	(0.00)
N1Hex-28-F	29.52	19.92	17.46	13.29	7.43	
	(−0.38)	(0.49)	(2.89)	(3.58)	(2.57)	
N0Hex-28-T	7.29					
N1Hex-28-T	7.18	0.00				
	(−8.07)	(0.00)				

0.68−0.69. Similar properties are also observed in the rectangular conformations. N0Hex-28-R-C (NICS = 46.98 ppm, ΔE_{HL} = 1.03 eV) and N1Hex-28-R-C (NICS = 20.96 ppm, ΔE_{HL} = 1.21 eV) have strong antiaromaticity and narrow HOMO−LUMO gaps, whereas N1Hex-28-R-N (NICS = 7.36 ppm, ΔE_{HL} = 1.47 eV) has nearly nonaromaticity and a relatively wide HOMO−LUMO gap. Again all three structures show similar HOMA indices of around 0.70−0.73. Not surprisingly, the twisted rectangular conformers exhibit much different aromatic characters. N0Hex-28-TR-C (−14.93 ppm) and N1Hex-28-TR-C (−10.98 ppm) show strong Möbius aromaticity, while N1Hex-28-TR-N (−6.78 ppm) shows moderate Möbius aromaticity. Weakening of aromatic character due to disruption of the annulenic circuit was also observed in the Hückel aromatic N-confused porphyrin.[26] Apparently larger HOMA indices are obtained for N0Hex-28-TR-C (0.8183) and N1Hex-28-TR-C (0.8136), which are consistent with their aromatic character. In addition, N1Hex-28-TR-N (0.7466) has an intermediate HOMA index between those of Möbius aromatic conformers and Hückel antiaromatic conformers. As expected from their strong or moderate aromaticity, the twisted rectangular conformers show much wider HOMO−LUMO gaps of 1.95 eV (N0Hex-28-TR-C), 1.79 eV (N1Hex-28-TR-C), and 1.73 eV (N1Hex-28-TR-N). The figure-eight conformers show nonaromatic character. The NICS values of N0Hex-28-F-C (7.80 ppm), N1Hex-28-F-C (2.30 ppm), and N1Hex-28-F-N (−0.79 ppm) are close to zero. The HOMA indices of the figure-eight conformers are the smallest among those of the five conformers (0.64−0.67), and the HOMO−LUMO gaps are between those of Möbius aromatic and Hückel antiaromatic [28]hexaphyrins (1.4−1.6 eV). Finally, the triangular conformers show properties similar to those of the dumbbell and rectangular conformers. N0Hex-28-T-C (NICS = 17.22 ppm, ΔE_{HL} = 1.31 eV) and N1Hex-28-T-C (NICS = 18.41 ppm, ΔE_{HL} = 1.24 eV) show moderate antiaromatic character and narrow HOMO−LUMO gaps, while N1Hex-28-

dx.doi.org/10.1021/jo401531w | J. Org. Chem. 2013, 78, 9317−9327

T-C (NICS = 9.15 ppm, ΔE_{HL} = 1.39 eV) has weak antiaromaticity and a relatively wide HOMO−LUMO gap.

In short, the NICS values are useful in evaluating the aromaticity of [28]hexaphyrins. The aromatic [28]hexaphyrins have larger HOMA indices of around 0.8, and the nonaromatic or antiaromatic [28]hexaphyrins have smaller HOMA indices in the region of 0.65−0.7. Thus, it would be difficult to distinguish between nonaromatic and antiaromatic [28]hexaphyrins only from HOMA analyses. On the other hand, the HOMO−LUMO gap becomes a good indicator. The aromatic [28]hexaphyrins have large ΔE_{HL} values of 1.8−2.0 eV, the antiaromatic [28]hexaphyrins have small ΔE_{HL} values of 1.0−1.3 eV, and the nonaromatic [28]hexaphyrins have medium ΔE_{HL} values of 1.4−1.6 eV. When singly N-confused [28]hexaphyrins have completed annulenic circuits, their aromatic characters are similar to those of regular [28]-hexaphyrins. Once the annulenic circuits are disrupted, their aromaticity or antiaromaticity becomes weaker and the molecules exhibit nonaromatic properties.

To check the relationship between orbital degeneracy and aromaticity in [28]hexaphyrins, the energies of the HOMO, HOMO − 1, LUMO, and LUMO + 1 are summarized in Figure 8. In the Möbius aromatic twisted rectangular conformers, the HOMOs and LUMOs are nearly degenerate as in the case of standard Hückel aromatic compounds. In all of the other structures, orbital degeneracy is completely lost, which is typical for nonaromatic or Hückel antiaromatic compounds. No remarkable change is observed simply due to confusion, but disruption of annulenic circuits causes a light loss of orbital degeneracy in the twisted rectangular conformation and a small gain of orbital degeneracy in the other conformations, which is consistent with the aromaticity of [28]hexaphyrins discussed above.

Effect of Confusion on Relative Stability. To evaluate the effect of confusion on stability, the relative energies of regular and singly N-confused [28]hexaphyrins with the same conformation and same N_H values are summarized in Table 3. The values in parentheses indicate the relative energies with correction by the N_H values based on the regression lines in Figures 6 and 7. Representative NH tautomers corresponding to Table 3 are shown in Figure 9. In the rectangular form, regular and singly N-confused [28]hexaphyrins showed similar relative stabilities. Thus, pure confusion does not affect the relative stability in antiaromatic [28]hexaphyrin frameworks. Meanwhile, regular [28]hexaphyrins are slightly more stable than singly N-confused [28]hexaphyrins by 1−4 kcal/mol in the twisted rectangular conformers. Confusion causes alteration in the [28]annulenic circuit pathway, which might have a slight destabilization effect on Möbius aromatic hexaphyrins. When the imino-type pyrrole is confused, the [28]annulenic circuit is disrupted as illustrated by the dumbbell and figure-eight conformers. In such cases, the regular [28]hexaphyrins are more stable than the singly N-confused [28]hexaphyrins by 3−5 kcal/mol. Thus, completion of the [28]annulenic circuit might stabilize the hexaphyrin macrocycles compared to the disrupted one even though they are antiaromatic.

The effect of the position and direction of the N-confused pyrrole in Möbius aromatic [28]hexaphyrins was also examined from the viewpoints of relative energies and aromaticity. The relative energies and the NICS values for the regular and singly N-confused [28]hexaphyrins with the twisted rectangular structure possessing a complete annulenic circuit are listed in Figure 10. To exclude the effect of intramolecular hydrogen

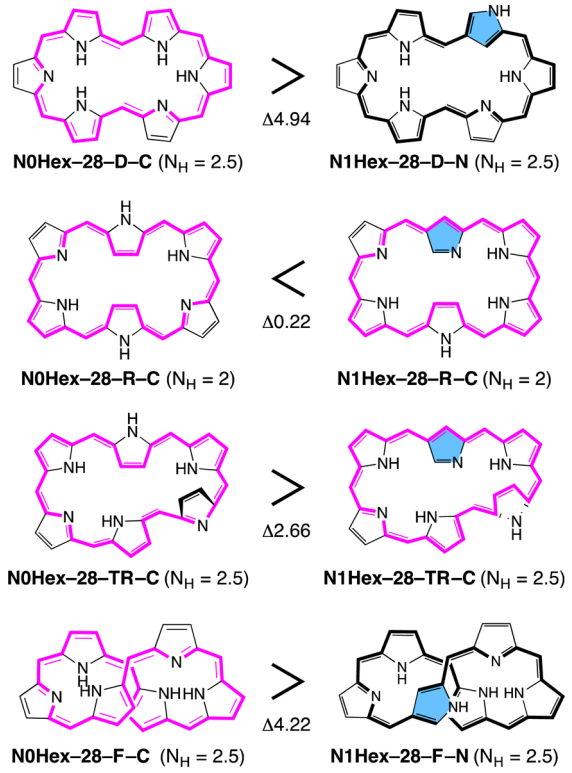

Figure 9. Comparison of relative energies (kcal/mol) between the representative NH tautomers of regular and singly N-confused [28]hexaphyrins shown in Table 3.

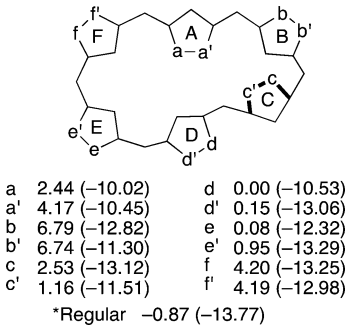

Figure 10. Relative energies (kcal/mol) and NICS values (in parentheses, ppm) of [28]hexaphyrins with N_H = 1 possessing a complete [28]annulenic circuit. Uncapitalized letters indicate the position of the nitrogen atom of the singly N-confused [28]-hexaphyrin.

bonds, the NH tautomers with the same N_H values of 1 are selected. When ring D or E was confused, the energy losses from the regular [28]hexaphyrin were less than 2 kcal/mol. Confusion at ring A or C caused moderate destabilization by 2−5 kcal/mol, and that at ring B or F caused considerable destabilization by 5−8 kcal/mol. Since no significant difference or reasonable trend was observed in the NICS values depending on the position of the N-confused pyrrole ring, the energy difference could be explained by the interaction and repulsion inside the macrocycle. When ring B or F was confused, CH···CH repulsion with ring A occurred inside the macrocycle, which would explain the considerable destabilization. When ring A was confused, CH···N interaction with ring B or F was replaced by N···N repulsion (repulsion between lone pairs), which would cause slight destabilization. In the case

dx.doi.org/10.1021/jo401531w | J. Org. Chem. 2013, 78, 9317−9327

of confusion at ring C, NH···NH repulsion with ring B was replaced by CH···NH repulsion, which might be thermodynamically unfavorable within the twisted rectangular skeleton.

Interconversion Pathway among Conformers. A conformational study on singly N-confused [28]hexaphyrins gives important information on the interconversion pathways among conformers (Scheme 1). The triangular conformer is drawn upside down for uniformity with the direction of the N-confused pyrrole. During the optimization of singly N-confused [28]hexaphyrin conformers, no local minimum was found in some NH tautomers. Rather, they were transformed into the other conformers after structural optimization, which would imply interconversion between the conformers. The figure-eight conformers were often unstable and readily converted into the known twisted rectangular conformer (twelve examples) or a twisted dumbbell conformer (four examples). The twisted dumbbell conformer was accidentally found through this study. The structure of the twisted dumbbell conformer (Figure 11a) can be constructed by rotating one pyrrole ring along the long axis of the dumbbell conformer. Thus, it is the intermediate structure between the dumbbell and figure-eight conformers. The twisted rectangular conformer did not have a local minimum occasionally and was converted into the standard rectangular conformer (six examples).[27] Accordingly, the dumbbell and rectangular conformers could be transformed through the figure-eight conformer, though the direct conversion between the dumbbell and rectangular conformers cannot be excluded at all. Similarly, transient structures between the rectangular and triangular conformers could be postulated by analogy. Namely, rotation of the right middle pyrrole in the triangular conformer gives a twisted triangular conformer, and further rotation of that pyrrole gives a semicircular conformer. Alternatively, rotation of the left lower pyrrole in the twisted rectangular conformer gives the semicircular conformer. Both postulated conformations were obtained as optimized structures from the arbitrarily constructed starting structures (Figure 11b,c). The proposed interconversion pathway for singly N-confused [28]hexaphyrins could be adaptable for regular [28]hexaphyrins. Importantly, such transformations during the structural optimization were never observed in regular [28]hexaphyrins. Hence, a confusion strategy on expanded porphyrins might be a uniquely effective way to obtain deep insight into their conformations even in theoretical studies.

Scheme 1. Possible Conformational Transformations in the Singly N-Confused [28]Hexaphyrin

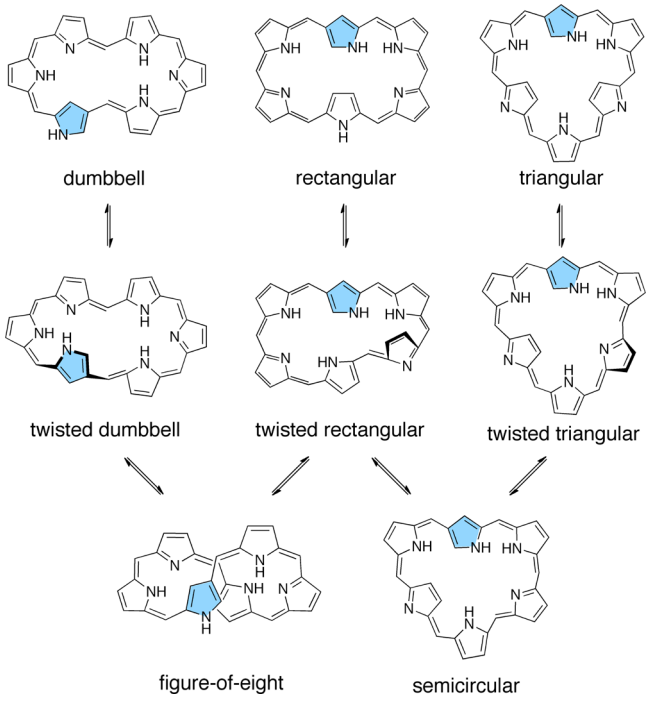

The twisted dumbbell conformer is another possible structure of a Möbius aromatic [28]hexaphyrin. The representative optimized structure of the twisted dumbbell conformer (denoted as N1Hex-28-TD-N) is shown in Figure 11a. The right part is nearly planar and resembles the standard dumbbell conformation. The pyrrole ring at the lower left is inverted, and accordingly, the adjacent pyrrole ring is tilted significantly. On the basis of the structure of N1Hex-28-TD-N, N0Hex-28-TD-C and N1Hex-28-TD-C were constructed and optimized to obtain the local minimum structures. The NH protons were arbitrarily placed. The NICS values and orbital energies of three structures are summarized in Figure 12. Expectedly, strong Möbius aromaticity is observed for N0Hex-28-TD-C (−13.19 ppm) and N1Hex-28-TD-C (−12.79 ppm), while moderate Möbius aromaticity is observed for N1Hex-28-TD-N (−5.77 ppm), similarly to the case of twisted rectangular structures. The degree of orbital degeneracy and HOMO−LUMO gaps are also similar to those of the twisted rectangular conformers and consistent with their aromaticity. Similarly, the twisted triangular conformer with the [28]annulenic circuit (N1Hex-28-TT-C) shows Möbius aromaticity (NICS = −9.34 ppm), and that without the [28]annulenic circuit (N1Hex-28-TT-N) shows moderate Möbius aromaticity (NICS = −6.44

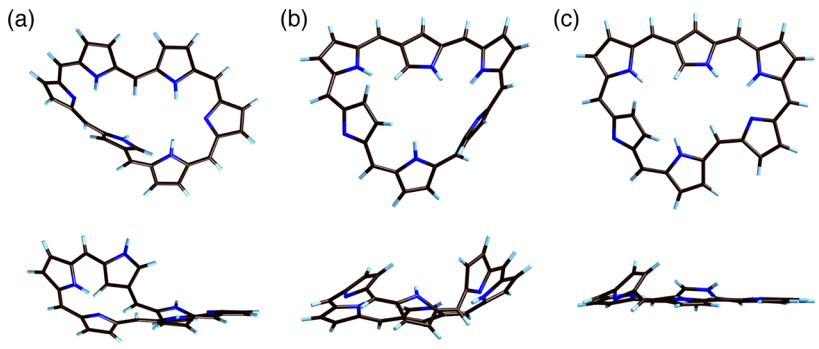

Figure 11. Top and side views of the (a) twisted dumbbell conformer, (b) twisted triangular conformer, and (c) semicircular conformer.

dx.doi.org/10.1021/jo401531w | J. Org. Chem. 2013, 78, 9317−9327

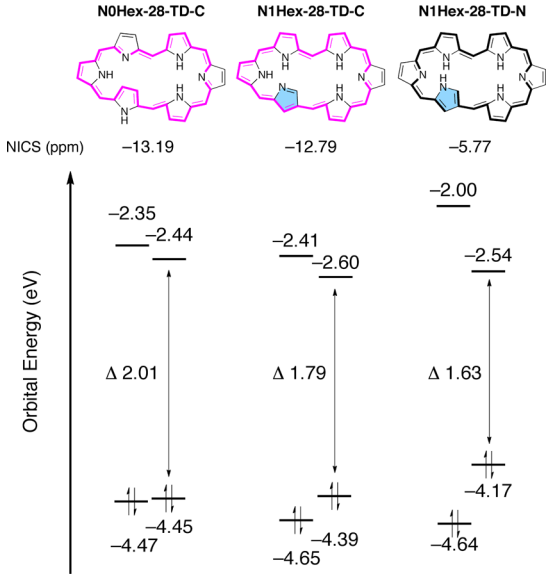

Figure 12. NICS values and orbital energies for the twisted dumbbell conformers.

ppm) (Figure S1, Supporting Information). In addition, the semicircular conformer shows nearly nonaromatic character (N1Hex-28-SC-C, NICS = 9.95 ppm; N1Hex-28-SC-N, NICS = 5.05 ppm), similarly to the figure-eight conformer (Figure S2, Supporting Information).

Effect of *meso*-Pentafluorophenyl Groups. Since *meso*-hexakis(pentafluorophenyl) derivatives were used in a large part of the experimental study on hexaphyrins,[28] the effect of *meso*-pentafluorophenyl groups on the relative energy was examined (Table 4). The relative energy among five regular [28]-hexaphyrins is denoted as ΔE_{reg}, and that among ten singly N-confused [28]hexaphyrins is denoted as ΔE_{conf}. In the regular *meso*-hexakis(pentafluorophenyl) [28]hexaphyrins, the order of thermodynamic stability was F > TR > D > R > T, while that in unsubstituted [28]hexaphyrins was D > TR > R > F > T. The order of relative stability in unsubstituted singly N-confused [28]hexaphyrins was R > D > TR > F > T, which changed to TR > F > R > T > D by introducing *meso*-pentafluorophenyl groups. Although small differences were found, the effect of *meso*-pentafluorophenyl groups was almost the same in regular and singly N-confused [28]hexaphyrins. Besides this, the existence or absence of a complete [28]annulenic circuit did not influence the effect of *meso*-pentafluorophenyl (C_6F_5) groups. Plausible effects imposed by *meso*-C_6F_5 groups would be (1) transannular repulsion between the two C_6F_5 groups, (2) transannular repulsion between the C_6F_5 group and the pyrrole rings, and (3) steric repulsion between the *o*-fluoro atoms and the pyrrole rings. The dumbbell conformer should be destabilized by the transannular repulsion between the two C_6F_5 groups inside the macrocycles. The transannular repulsion between the C_6F_5 group and the pyrrole rings would be expected in nonplanar structures such as the twisted rectangular and figure-eight conformers, but the effect might be small because of the flexibility of the parent [28]hexaphyrin skeleton. The steric repulsion between the *o*-fluoro atoms and the pyrrole rings would be significant when the parent hexaphyrin skeleton is planar (dumbbell, rectangular, and triangular), while such repulsion might be less in the nonplanar case. As a result, the nonplanar conformers (twisted rectangular and figure-eight) became relatively stable by introducing *meso*-C_6F_5 groups to the [28]hexaphyrins. Actually, the twisted rectangular structures were experimentally observed in both regular and singly N-confused *meso*-hexakis(pentafluorophenyl)[28]-hexaphyrins. Although the reason for preferential stability in the figure-eight conformers was unclear, the interactions between the C_6F_5 groups and the hexaphyrin π-orbitals might be overestimated due to the basis set superposition error.[29]

Comparison between [28]Hexaphyrins and [26]-Hexaphyrins. Finally, the effect of each factor on [28]-hexaphyrins is compared with that on [26]hexaphyrins briefly.[8] Intramolecular hydrogen bonds are the critical factor governing the conformations in both [28]hexaphyrins and [26]-hexaphyrins, where one hydrogen bond stabilizes the macrocycle by ca. 10 kcal/mol. Ring strain significantly affects the relative stability of [26]hexaphyrin conformers, while it becomes less important in the case of [28]hexaphyrins. Aromaticity and orbital energies are highly dependent on the conformations in [28]hexaphyrins, whereas only small changes are observed in [26]hexaphyrins. The effect of *meso*-aryl groups is similar in both [28]hexaphyrins and [26]hexaphyrins.

CONCLUSION

In this paper, the structures and electronic states of regular and singly N-confused [28]hexaphyrin conformers and NH tautomers were investigated with the aid of DFT calculations. Important findings in this study are summarized as follows:

(1) Intramolecular hydrogen bonds are the critical factor governing the conformation of [28]hexaphyrins. One hydrogen bond stabilizes the macrocycle by ca. 10 kca/mol.
(2) Ring strain is less effective than in the case of [26]hexaphyrins.
(3) The dumbbell, rectangular, and triangular conformers are Hückel antiaromatic, the twisted rectangular conformer is Möbius aromatic, and the figure-eight conformer is nonaromatic.
(4) The NICS values and orbital energies are useful indicators to analyze aromaticity, while the HOMA indices are partially effective.
(5) Disruption of the antiaromatic [28]annulenic circuit causes destabilization by 3−5 kcal/mol.

Table 4. Relative Energies (kcal/mol) among Conformers for Regular and Singly N-Confused *meso*-Hexakis(pentafluorophenyl)[28]hexaphyrins

sructure	ΔE_{reg}	sructure	ΔE_{conf}	sructure	ΔE_{conf}
N0Hex-28-D-C	6.28	N1Hex-28-D-C	14.91	N1Hex-28-D-N	16.18
N0Hex-28-R-C	13.72	N1Hex-28-R-C	10.28	N1Hex-28-R-N	7.49
N0Hex-28-TR-C	1.27	N1Hex-28-TR-C	0.00	N1Hex-28-TR-N	0.24
N0Hex-28−F-C	0.00	N1Hex-28−F-C	8.07	N1Hex-28−F-N	1.42
N0Hex-28-T-C	22.39	N1Hex-28-T-C	12.82	N1Hex-28-T-N	13.57

dx.doi.org/10.1021/jo401531w | J. Org. Chem. 2013, 78, 9317−9327

(6) Possible conformational interconversion pathways for [28]hexaphyrins are proposed, where the Möbius aromatic twisted dumbbell conformer and twisted triangular conformer are postulated.

The above information would be beneficial for the development of expanded porphyrin chemistry as well as confusion chemistry. Also the present study contributes further understanding of aromaticity in porphyrins and related macrocyclic compounds.[30]

■ ASSOCIATED CONTENT

Supporting Information

Orbital energies of twisted triangular and semicircular conformers, chemical structures, and Cartesian coordinates for all the optimized structures. This material is available free of charge via the Internet at http://pubs.acs.org.

■ AUTHOR INFORMATION

Corresponding Author

*E-mail: hfuruta@cstf.kyushu-u.ac.jp.

Notes

The authors declare no competing financial interest.

■ ACKNOWLEDGMENTS

The present work was supported by Grants-in-Aid for Young Scientists (25870504) to M.T. and on Innovative Areas (231087015) to H.F. from the Ministry of Education, Culture, Sports, Science and Technology of Japan.

■ REFERENCES

(1) (a) Shelnutt, J. A.; Song, X.-Z.; Ma, J.-G.; Jia, S.-L.; Jentzen, W.; Medforth, C. J. *Chem. Soc. Rev.* **1998**, *27*, 31−41. (b) Senge, M. O.; Medforth, C. J.; Forsyth, T. P.; Lee, D. A.; Olmstead, M. M.; Jentzen, W.; Pandey, R. K.; Shelnutt, J. A.; Smith, K. M. *Inorg. Chem.* **1997**, *36*, 1149−1163.

(2) (a) Ghosh, A. *Angew. Chem., Int. Ed.* **2004**, *43*, 1918−1931. (b) Sessler, J. L.; Seidel, D. *Angew. Chem., Int. Ed.* **2003**, *42*, 5134−5175. (c) Jasat, A.; Dolphin, D. *Chem. Rev.* **1997**, *97*, 2267−2340. (d) Saito, S.; Osuka, A. *Angew. Chem., Int. Ed.* **2011**, *50*, 4342−4373. (e) Stępień, M.; Sprutta, N.; Latos-Grażyński, L. *Angew. Chem., Int. Ed.* **2011**, *50*, 4288−4340. (f) Misra, R.; Chandrashekar, T. K. *Acc. Chem. Res.* **2008**, *41*, 265−279.

(3) Lim, J. M.; Lee, J. S.; Chung, H. W.; Bahng, H. W.; Yamaguchi, K.; Toganoh, M.; Furuta, H.; Kim, D. *Chem. Commun.* **2010**, *46*, 4357−4359.

(4) Toganoh, M.; Furuta, H. *Chem. Commun.* **2012**, *48*, 937−954.

(5) (a) Gokulnath, A.; Nishimura, K.; Toganoh, M.; Mori, S.; Furuta, H. *Angew. Chem., Int. Ed.* **2013**, *52*, 6940−6943. (b) Gokulnath, S.; Toganoh, M.; Yamaguchi, K.; Mori, S.; Uno, H.; Furuta, H. *Dalton. Trans.* **2012**, *41*, 6283−6290. (c) Gokulnath, S.; Yamaguchi, K.; Toganoh, M.; Mori, S.; Uno, H.; Furuta, H. *Angew. Chem., Int. Ed.* **2011**, *50*, 2302−2306.

(6) (a) Srinivasan, A.; Ishizuka, T.; Osuka, A.; Furuta, H. *J. Am. Chem. Soc.* **2003**, *125*, 878−879. (b) Suzuki, M.; Yoon, M.-C.; Kim, D. Y.; Kwon, J. H.; Furuta, H.; Kim, D.; Osuka, A. *Chem.—Eur. J.* **2006**, *12*, 1754−1759.

(7) Xie, Y.-S.; Yamaguchi, K.; Toganoh, M.; Uno, H.; Suzuki, M.; Mori, S.; Saito, S.; Osuka, A.; Furuta, H. *Angew. Chem., Int. Ed.* **2009**, *48*, 5496−5499.

(8) Toganoh, M.; Furuta, H. *J. Org. Chem.* **2010**, *75*, 8213−8223.

(9) (a) Yamamoto, Y.; Yamamoto, A.; Furuta, S.; Horie, M.; Kodama, M.; Sato, W.; Akiba, K.; Tsuzuki, S.; Uchimaru, T.; Hashizume, D.; Iwasaki, F. *J. Am. Chem. Soc.* **2005**, *127*, 14540−14541. (b) Yamamoto, Y.; Hirata, Y.; Kodama, M.; Yamaguchi, T.; Matsukawa, S.; Akiba, K.; Hashizume, D.; Iwasaki, F.; Muranaka, A.; Uchiyama, M.; Chen, P.; Kadish, K. M.; Kobayashi, N. *J. Am. Chem. Soc.* **2010**, *132*, 12627−12638. (c) Kakui, T.; Sugawara, S.; Hirata, Y.; Kojima, S.; Yamamoto, Y. *Chem.—Eur. J.* **2011**, *17*, 7768−7771.

(10) Liu, C.; Shen, D.-M.; Chen, Q.-Y. *J. Am. Chem. Soc.* **2007**, *129*, 5814−5815.

(11) Muranaka, A.; Matsushita, O.; Yoshida, K.; Mori, S.; Suzuki, M.; Furuyama, T.; Uchiyama, M.; Osuka, A.; Kobayashi, N. *Chem.—Eur. J.* **2009**, *15*, 3744−3751.

(12) (a) Shimizu, S.; Anand, V. G.; Taniguchi, R.; Furukawa, K.; Kato, T.; Yokoyama, T.; Osuka, A. *J. Am. Chem. Soc.* **2004**, *126*, 12280−12281. (b) Mori, S.; Shimizu, S.; Shin, J.-Y.; Osuka, A. *Inorg. Chem.* **2007**, *46*, 4374−4376.

(13) Rath, H.; Aratani, N.; Lim, J. M.; Lee, J. S.; Kim, D.; Shinokubo, H.; Osuka, A. *Chem. Commun.* **2009**, 3762−3764.

(14) Sankar, J.; Mori, S.; Saito, S.; Rath, H.; Suzuki, M.; Inokuma, Y.; Shinokubo, H.; Kim, K. S.; Yoon, Z. S.; Shin, J.-Y.; Lim, J. M.; Matsuzaki, Y.; Matsushita, O.; Muranaka, A.; Kobayashi, N.; Kim, D.; Osuka, A. *J. Am. Chem. Soc.* **2008**, *130*, 13568−13579.

(15) Tokuji, S.; Shin, J.-Y.; Kim, K. S.; Lim, J. M.; Youfu, K.; Saito, S.; Kim, D.; Osuka, A. *J. Am. Chem. Soc.* **2009**, *131*, 7240−7241.

(16) Koide, T.; Youfu, K.; Saito, S.; Osuka, A. *Chem. Commun.* **2009**, 6047−6049.

(17) Allan, C. S. M.; Rzepa, H. S. *J. Org. Chem.* **2008**, *73*, 6615−6622.

(18) Fliegl, H.; Sundholm, D.; Taubert, S.; Pichierri, F. *J. Phys. Chem. A* **2010**, *114*, 7153−7161.

(19) Frisch, M. J.; Trucks, G. W.; Schlegel, H. B.; Scuseria, G. E.; Robb, M. A.; Cheeseman, J. R.; Scalmani, G.; Barone, V.; Mennucci, B.; Petersson, G. A.; Nakatsuji, H.; Caricato, M.; Li, X.; Hratchian, H. P.; Izmaylov, A. F.; Bloino, J.; Zheng, G.; Sonnenberg, J. L.; Hada, M.; Ehara, M.; Toyota, K.; Fukuda, R.; Hasegawa, J.; Ishida, M.; Nakajima, T.; Honda, Y.; Kitao, O.; Nakai, H.; Vreven, T.; Montgomery, Jr., J. A.; Peralta, J. E.; Ogliaro, F.; Bearpark, M.; Heyd, J. J.; Brothers, E.; Kudin, K. N.; Staroverov, V. N.; Kobayashi, R.; Normand, J.; Raghavachari, K.; Rendell, A.; Burant, J. C.; Iyengar, S. S.; Tomasi, J.; Cossi, M.; Rega, N.; Millam, J. M.; Klene, M.; Knox, J. E.; Cross, J. B.; Bakken, V.; Adamo, C.; Jaramillo, J.; Gomperts, R.; Stratmann, R. E.; Yazyev, O.; Austin, A. J.; Cammi, R.; Pomelli, C.; Ochterski, J. W.; Martin, R. L.; Morokuma, K.; Zakrzewski, V. G.; Voth, G. A.; Salvador, P.; Dannenberg, J. J.; Dapprich, S.; Daniels, A. D.; Farkas, Ö.; Foresman, J. B.; Ortiz, J. V.; Cioslowski, J.; Fox, D. J. *Gaussian 09*, revision C.01; Gaussian, Inc.: Wallingford, CT, 2009.

(20) (a) Becke, A. D. *J. Phys. Chem.* **1993**, *98*, 5648−5652. (b) Lee, C.; Yang, W.; Parr, R. G. *Phys. Rev. B* **1988**, *37*, 785−789. (c) Vosko, S. H.; Wilk, L.; Nusair, M. *Can. J. Phys.* **1980**, *58*, 1200−1211. (d) Stephens, P. J.; Devlin, F. J.; Chabalowski, C. F.; Frisch, M. J. *J. Phys. Chem.* **1994**, *98*, 11623−11627.

(21) (a) Schleyer, P. v. R.; Maerker, C.; Dransfeld, A.; Jiao, H.; Hommes, N. v. E. *J. Am. Chem. Soc.* **1996**, *118*, 6317−6318. (b) Chen, Z.; Wannere, C. S.; Corminboeuf, C.; Puchta, R.; Schleyer, P. v. R. *Chem. Rev.* **2005**, *105*, 3842−3888.

(22) (a) Sessler, J. L.; Seidel, D.; Vivian, A. E.; Lynch, V.; Scott, B. L.; Keogh, D. W. *Angew. Chem., Int. Ed.* **2001**, *40*, 591−594. (b) Shimizu, S.; Taniguchi, R.; Osuka, A. *Angew. Chem., Int. Ed.* **2005**, *44*, 2225−2229. (c) Pushpan, S. K.; Anand, V. R. G.; Venkatraman, S.; Srinivasan, A.; Gupta, A. K.; Chandrashekar, T. K. *Tetrahedron Lett.* **2001**, *42*, 3391−3394. (d) Sessler, J. L.; Seidel, D.; Bucher, C.; Lynch, V. *Chem. Commun.* **2000**, 1473−1474. (e) Zhu, X.-J.; Fu, S.-T.; Wong, W.-K.; Guo, J.-P.; Wong, W.-Y. *Angew. Chem., Int. Ed.* **2006**, *45*, 3150−3154.

(23) A Möbius ring is usually created by cutting a normal ring and subsequently rejoining the ends of the strip with a half-twist. Cutting the macrocycle does not require that it be in the twisted rectangular form.

(24) (a) Eisler, S.; McDonald, R.; Loppnow, G. R.; Tykwinski, R. R. *J. Am. Chem. Soc.* **2000**, *122*, 6917−6928. (b) Brubaker, G. R.; Johnson, D. W. *Inorg. Chem.* **1984**, *23*, 1591−1595.

(25) (a) Krygowski, T. M.; Cyrański, M. *Tetrahedron* **1996**, *52*, 10255−10264. (b) Krygowski, T. M.; Cyrański, M. *Chem. Rev.* **2001**,

101, 1385−1420. (c) Stanger, A. *J. Am. Chem. Soc.* **1998**, *120*, 12034−12040.
(26) (a) Furuta, H.; Ishizuka, T.; Osuka, A.; Dejima, H.; Nakagawa, H.; Ishikawa, Y. *J. Am. Chem. Soc.* **2001**, *123*, 6207−6208. (b) Toganoh, M.; Yamamoto, T.; Hihara, T.; Akimaru, H.; Furuta, H. *Org. Biomol. Chem.* **2012**, *10*, 4367−4374. (c) Toganoh, M.; Furuta, H. *J. Phys. Chem. A* **2009**, *113*, 13953−13963.
(27) Alonso, M.; Geerlings, P.; De Proft, F. *Chem.—Eur. J.* **2012**, *18*, 10916−10928.
(28) (a) Neves, M. G. P. M. S.; Martins, R. M.; Tome, A. C.; Silvestre, A. J. D.; Silva, A. M. S.; Felix, V.; Drew, M. G. B.; Cavaleiro, J. A. S. *Chem. Commun.* **1999**, 385−386. (b) Shin, J.-Y.; Furuta, H.; Yoza, K.; Igarashi, S.; Osuka, A. *J. Am. Chem. Soc.* **2001**, *123*, 7190−7191.
(29) Gutowski, M.; Chałasiński, G. *J. Chem. Phys.* **1993**, *98*, 5540−5554.
(30) Wu, J. I.; Fernandez, I.; Schleyer, P. v. R. *J. Am. Chem. Soc.* **2013**, *135*, 315−321.

dx.doi.org/10.1021/jo401531w | *J. Org. Chem.* 2013, 78, 9317−9327